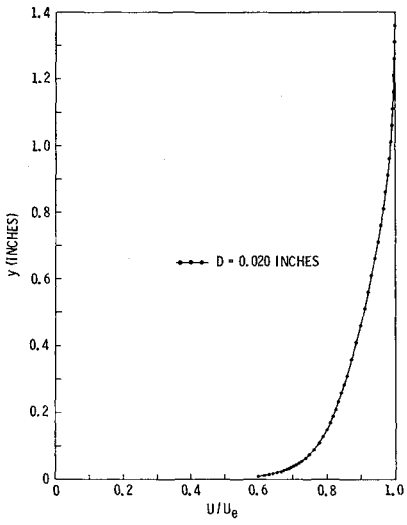


**Fig. 2 Velocity distribution—0.020-in. pitot tube.**

insured that contact between the tube and wall occurred at the shoulder of the bevel. Very light contact could be detected by a change in electrical resistance with no bending of the tube. A micrometer attached to the tube-traversing mechanism could be set at zero at this point.

Velocities in the boundary layer were determined from pitot pressure and tunnel supply pressure assuming constant total temperature. The data for all five surveys are tabulated in Ref. 4. The velocity profiles shown on Figs. 2 and 3 were obtained with the $D = 0.020$-in. and $D = 0.095$-in. tubes. The curve faired through the $D = 0.020$-in. data of Fig. 2 is reproduced on Fig. 3 for comparison with the $D = 0.095$-in. data. The $D = 0.020$-in. tube gives very nearly the correct results. Figure 3 demonstrates that the interference effects with a tube as large as $D = 0.095$ in. are quite small.

The boundary-layer momentum thickness, $\theta$, and displacement thickness, $\delta^*$, were determined from the data for each survey. In order to carry the integrations all the way to the wall, the velocity was assumed to vary with the $\frac{1}{7}$th root of distance in the region between the wall and the first survey point. Values of $\theta$ and $H = \delta^*/\theta$ from Ref. 4, nondimensionalized by values for zero tube diameter, are plotted on Fig. 4. Even with the largest tube (about 25% of the boundary-layer thickness), the error in $\theta$ is only 2% and the error in $H$ only 1%. In plotting the data from Ref. 4 vs $D/\delta$, it should be noted that $\delta$ was taken as the thickness of a boundary layer with the entire velocity profile given by a $\frac{1}{7}$th-root distribution. This fictitious boundary layer had the same $\theta$ as the boundary layer surveyed.

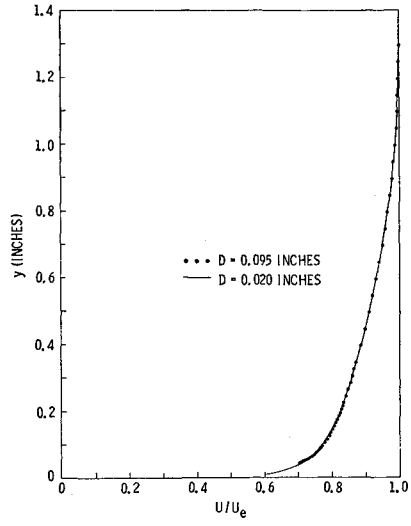


**Fig. 3 Velocity distribution—comparison of 0.020-in. and 0.095-in. pitot tubes.**

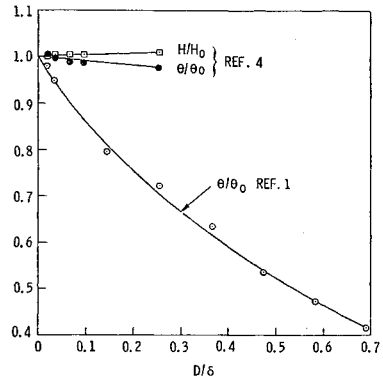


**Fig. 4 Effect of pitot tube size on $\theta$ and $H$.**

The effect of tube diameter on $\theta$ given by Allen in Ref. 1 is much greater than the effect given in Ref. 4. Allen's data were also obtained by surveying a zero heat-transfer turbulent boundary layer with an edge Mach number of 2.0. The great difference in the results can be seen on Fig. 4. This must be due to the differences in the pitot tube and support configurations. Allen's pitot tubes were also circular in cross section, but the tips were not beveled. The support used by Allen was circular in cross section with each pitot tube extending upstream for a distance of three support diameters. The difference in data from the two sources demonstrates that the tube and support configuration design given in Ref. 4 was successful in minimizing interference effects. It should be noted that, since the tube tips were beveled, it might be argued that the data on Fig. 4 for $\theta$ and $H$ from Ref. 4 should be plotted vs $d/\delta$, where $d$ is the tube inside diameter. The interference for the tube and support configuration from Ref. 4 is so small that the comparison with the data from Ref. 1 is hardly affected.

Allen analyzed his data to obtain pitot tube displacement distributions through the boundary layer. These distributions are given in Refs. 1 and 2. The data obtained by E. C. Young and the author are completely tabulated in Ref. 4 and could be used to obtain displacement distributions. These displacements will be small compared to those obtained by Allen.

### References

[1] Allen, J. M., "Pitot-Probe Displacement in a Supersonic Turbulent Boundary Layer," TN D-6759, April 1972, NASA.

[2] Allen, J. M., "Impact Probe Displacement in a Supersonic Turbulent Boundary Layer," *AIAA Journal*, Vol. 10, No. 4, April 1972, pp. 555–557.

[3] Wilson, R. E., "Turbulent Boundary-Layer Characteristics at Supersonic Speeds—Theory and Experiment," *Journal of Aeronatuical Sciences*, Vol. 17, No. 9, Sept. 1950, pp. 585–594.

[4] Wilson, R. E. and Young, E. C., "Aerodynamic Interference of Pitot Tubes in a Turbulent Boundary Layer at Supersonic Speed," CF-1351, Rept. 228, Dec. 1959, Defense Research Lab., Univ. of Texas, Austin, Texas.

# Vibration of Orthotropic Circular Plates with a Concentric Isotropic Core

H. K. Woo,* P. G. Kirmser,† and C. L. Huang‡
*Kansas State University, Manhattan, Kansas*

In a recent Note[1] by the writers, it is proved that cylindrical orthotropy cannot exist at the center of a circular plate. In order to correct the orthotropic circular plate theory for this

Received March 15, 1973; revision received June 4, 1973.
Index category: Structural Dynamic Analysis.
* Graduate Research Assistant.
† Professor of Applied Mechanics.
‡ Associate Professor of Applied Mechanics. Member AIAA.

**Table 1 Axisymmetric frequency parameters $\lambda^{1/2} = (\rho h/D_r)^{1/2}a^2\omega$ for a clamped orthotropic circular plate with a concentric isotropic core**

| $\beta$ | $\lambda^{1/2}$ for values of $b/a$ | | | | |
|---|---|---|---|---|---|
| | 0.5 | 0.3 | 0.2 | 0.1 | 0.025 |
| 0.1 | 9.701 | 9.152 | 8.852 | 8.542 | 8.284 |
| 0.2 | 9.760 | 9.279 | 9.024 | 8.776 | 8.598 |
| 0.3 | 9.818 | 9.404 | 9.190 | 8.993 | 8.871 |
| 0.4 | 9.876 | 9.527 | 9.351 | 9.197 | 9.113 |
| 0.5 | 9.933 | 9.647 | 9.506 | 9.389 | 9.335 |
| 0.6 | 9.990 | 9.764 | 9.657 | 9.571 | 9.534 |
| 0.7 | 10.046 | 9.880 | 9.802 | 9.743 | 9.720 |
| 0.8 | 10.102 | 9.994 | 9.944 | 9.907 | 9.895 |
| 0.9 | 10.158 | 10.105 | 10.081 | 10.065 | 10.059 |
| 1.0 | 10.215 | 10.215 | 10.215 | 10.215 | 10.215 |
| 1.1 | 10.268 | 10.323 | 10.345 | 10.360 | 10.364 |
| 1.2 | 10.323 | 10.429 | 10.472 | 10.499 | 10.506 |
| 1.3 | 10.377 | 10.534 | 10.596 | 10.634 | 10.642 |
| 1.4 | 10.430 | 10.637 | 10.717 | 10.764 | 10.774 |
| 1.5 | 10.484 | 10.738 | 10.835 | 10.890 | 10.900 |
| 1.6 | 10.537 | 10.838 | 10.951 | 11.013 | 11.023 |
| 1.7 | 10.590 | 10.937 | 11.064 | 11.131 | 11.142 |
| 1.8 | 10.642 | 11.033 | 11.175 | 11.247 | 11.258 |
| 1.9 | 10.694 | 11.129 | 11.283 | 11.360 | 11.370 |
| 2.0 | 10.746 | 11.224 | 11.389 | 11.470 | 11.480 |

singularity in the material properties, it is proposed that the neighborhood of the center of the plate be treated as an isotropic core with an infinitesimal radius, as suggested by Carrier[2] for static problems, and Salzman and Patel[3] for dynamics problems. With this correction, the singular behavior at the center of the plate can be removed. It is our purpose in this Note to investigate the free vibrations of a cylindrically orthotropic circular plate with a concentric isotropic core. Both clamped and hinged circular plates are considered.

Each problem is described by two partial differential equations of the type shown in our previous Note,[1] holding with different values of the stiffness ratio parameter $\beta$ in the orthotropic and isotropic domains, and appropriate boundary conditions at the interfaces and edges of these domains.

Numerical solutions were obtained by the parallel shooting method[4] using a fourth-order Runge-Kutta procedure and making successive corrections by Newton's method. The theorem of Newton-Kantorovich[5] guarantees the convergence and uniqueness of the solutions. The variation of the natural frequency with the stiffness parameter $\beta$ was obtained by the continuation method of Ficken.[6]

**Table 2 Axisymmetric frequency parameters $\lambda^{1/2} = (\rho h/D_r)^{1/2}a^2\omega$ for a simply supported orthotropic circular plate with a concentric isotropic core**

| $\beta$ | $\lambda^{1/2}$ for values of $b/a$ | | | | |
|---|---|---|---|---|---|
| | 0.5 | 0.3 | 0.2 | 0.1 | 0.025 |
| 0.1 | 4.018 | 3.606 | 3.403 | 3.192 | 3.009 |
| 0.2 | 4.130 | 3.781 | 3.616 | 3.457 | 3.343 |
| 0.3 | 4.240 | 3.946 | 3.814 | 3.695 | 3.622 |
| 0.4 | 4.346 | 4.104 | 4.000 | 3.911 | 3.865 |
| 0.5 | 4.450 | 4.256 | 4.175 | 4.110 | 4.081 |
| 0.6 | 4.551 | 4.401 | 4.341 | 4.296 | 4.277 |
| 0.7 | 4.650 | 4.542 | 4.499 | 4.469 | 4.458 |
| 0.8 | 4.747 | 4.677 | 4.651 | 4.626 | 4.627 |
| 0.9 | 4.842 | 4.808 | 4.796 | 4.787 | 4.785 |
| 1.0 | 4.935 | 4.935 | 4.935 | 4.935 | 4.935 |
| 1.1 | 5.026 | 5.058 | 5.069 | 5.076 | 5.077 |
| 1.2 | 5.116 | 5.178 | 5.199 | 5.211 | 5.213 |
| 1.3 | 5.204 | 5.295 | 5.324 | 5.341 | 5.344 |
| 1.4 | 5.290 | 5.409 | 5.446 | 5.446 | 5.469 |
| 1.5 | 5.375 | 5.519 | 5.564 | 5.587 | 5.590 |
| 1.6 | 5.459 | 5.628 | 5.679 | 5.704 | 5.707 |
| 1.7 | 5.541 | 5.734 | 5.790 | 5.818 | 5.821 |
| 1.8 | 5.622 | 5.837 | 5.899 | 5.928 | 5.931 |
| 1.9 | 5.701 | 5.939 | 6.005 | 6.035 | 6.038 |
| 2.0 | 5.780 | 6.039 | 6.109 | 6.140 | 6.143 |

The numerical computation was carried out on an IBM 360/50 computer for both clamped and hinged circular orthotropic plates with concentric isotropic cores. The stiffness parameter was chosen to range from 0.1 to 2.0, and the ratio of the radius of isotropic core to the outer radius of the plate from 0.025 to 0.5. Numerical results are given in Tables 1 and 2 for clamped and hinged plates, respectively. The results show that the frequency parameter increases as the stiffness increases, which agrees with the conclusion given in our previous Note.[1] The numerical results obtained for the case of $R = 0.025$ give an excellent approximate solution for the vibration of an orthotropic circular plate. In addition, the results obtained for a circular plate with stiffness ratio parameter $\beta = 1$, which reduces the orthotropic plate to an isotropic one, agree with the classical results appearing in the literature.[7]

### References


[1] Kirmser, P. G., Huang, C. L., and Woo, H. K., "Vibration of Cylindrically Orthotropic Circular Plates," *AIAA Journal*, Vol. 10, No. 12, Dec. 1972, pp. 1690–1691.

[2] Carrier, G. F., "Stress Distributions in Cylindrically Aeolotropic Plates," *Journal of Applied Mechanics*, Vol. 65, 1943, pp. A117–A122.

[3] Salzman, A. P. and Patel, S. A., "Natural Frequencies of Orthotropic Circular Plates of Variable Thickness," PIBAL Rept. 68-8, April 1968, Polytechnic Inst. of Brooklyn, Brooklyn, N.Y.

[4] Keller, H. B., *Numerical Methods for Two-Point Boundary-Value Problems*, Blaisdell, Waltham, Mass., 1968, pp. 61–71.

[5] Kantorovich, L. V. and Akilov, G. P., *Functional Analysis in Normed Spaces*, MacMillan, New York, 1964, pp. 695–749.

[6] Ficken, F. A., "The Continuation Method for Functional Equations," *Comm. Pure Applied Mathematics*, Vol. 4, 1951, pp. 435–456.

[7] Leissa, A. W., *Vibration of Plates*, NASA SP-160, 1969, pp. 8–9.


# Buckling of Segments of Toroidal Shells


V. I. WEINGARTEN* AND D. R. VERONDA†
*University of Southern California, Los Angeles, Calif.*

AND

S. S. SAGHERA‡
*McDonnell Douglas Astronautics Company, Huntington Beach, Calif.*


### Introduction

SHELLS of double curvature are commonly used in aerospace and civil engineering structures. Buckling must be considered in the design of such shells. Many of the stability monographs and state-of-the-art papers[1–3] recommend using the curves published by Stein and McElman[4] for determining the buckling pressure of segments of toroidal and hyperboloidal shells of


Received December 8, 1972; revision received May 23, 1973. This research was supported under a National Science Foundation Grant GK 25136X.

Index category: Structural Stability Analysis.



* Professor, Department of Civil Engineering.

† Lecturer, Department of Civil Engineering; also Member of the Technical Staff, Hughes Aircraft Company, Fullerton, Calif.

‡ Engineer/Scientist Specialist, Structures Department.